Freezing of Tidal Flow in Lake Vallunden (Spitsbergen)

A. V. Marchenko[1,2,3], E. G. Morozov[4], A. V. Ivanov[5], T. G. Elizarova[5], and D. I. Frey[4]

[1] Svalbard University Center, Longyearbyen, Spitsbergen, Norway

[2] Zubov State Oceanographic Institute, Moscow, Russia

[3] Sustainable Arctic Marine and Coastal Technology (SAMCoT)), Centre for Research-Based Innovation (CRI), Norway

[4] Shirshov Institute of Oceanology, Russian Academy of Sciences, Moscow, Russia

[5] Keldysh Institute of Applied Mathematics, Russian Academy of Sciences, Moscow, Russia

Correspondence to: E.G. Morozov (egmorozov@mail.ru)

ABSTRACT

In March 2019, Lake Vallunden was surveyed to construct a chart of ice thickness. Lake Valunden is a lake in Spitsbergen at the top of the Van Mijen Fjord. The lake is approximately 1 km long, 600 m wide, and 10 m deep. It is connected to the Van Mijen Fjord by a channel 100 long and 10 m wide. The tides in the fjord are high; hence periodical tidal currents to the lake and from the lake exceed 1 m/s. In winter, the channel normally would be frozen, but due to the strong tides in the channel the water does not freeze. Instead, the water in the channel transports supercooled water and the corresponding frazil ice particles to Lake Vallunden. A strong tidal jet of ice-free water ~100 m long flows from the channel to the lake. The velocity of the jet decreases in the lake as the jet flows under ice. The current transports ice crystals and frazil ice, which freeze immediately around the place where the jet submerges under the ice, approximately at a distance of 100 m from the channel. The ice thickness in this region reaches 120 cm, whereas in the rest of the lake it is 70 cm. A mathematical model is suggested showing the velocity field of diverging and circulating tidal flow in the lake.

KEY WORDS: tidal current; Lake Vallunden; Spitsbergen; Van Mijen Fjord; freezing

1. INTRODUCTION

During recent years, scientists from the University Center in Svalbard have been studying properties of ice in Lake Vallunden in Spitsbergen and the relation of ice properties to the strong water exchange between the lake and Van Mijen Fjord. Lake Valunden is approximately 1200 m long and from 300 to 750 m wide [*Marchenko and Morozov*, 2016]. The bottom of the lake is almost flat and its mean depth is 10-11 m. A shallow channel (~1-2 m deep) connects the lake and the fjord. The channel is 100 m long and 10 m wide [*Marchenko and Morozov*, 2013]. In winter, the lake and fjord are covered with ice, but the channel sometimes remains ice-free even in very cold winters because of the strong tidal flow in the channel. The tidal oscillations of sea level in the fjord exceed ±1m. Due to strong variations in the sea level, the velocity of periodical tidal currents in the channel exceeds 1 m/s. If the channel is ice-free in winter, water temperature in the channel is close to freezing. It strongly cools while flowing along the channel. The jet from the channel continues into the lake and its velocity decreases in the lake approximately at a distance of 100-200 m from the channel. In 2019, field works were performed in the lake near the channel. A chart of the region is shown in Fig. 1. In our previous studies [*Marchenko and Morozov*, 2013; *Morozov et al.*, 2019] we made measurements in the strong tidal flow in the channel. This tidal flow generates short period internal waves [Morozov and Pisarev, 2002; Morozov et al., 2019].

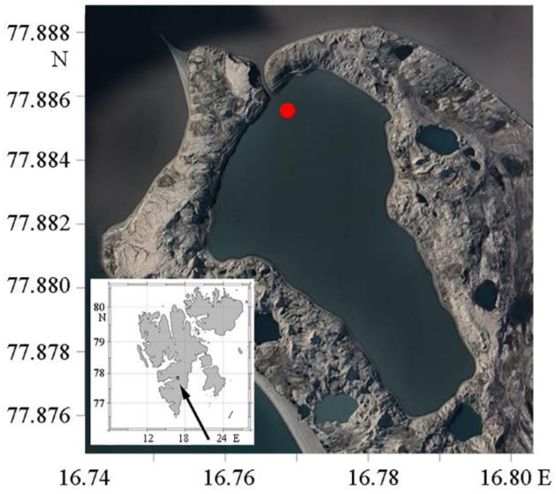

Fig. 1. Chart of Lake Valunden (satellite photo). The red dot indicates location of the experiment. The inset shows location of the lake in Spitsbergen.

Our research is aimed at investigating the influence of the strong tidal current on water freezing. The measured thickness of ice near the channel was one and a half times thicker than in the rest of the lake. The strong tidal currents in the strait continue into the lake preventing ice freezing along a narrow strip of the continuation of current from the channel, but ice thickness increases at the end of this strip.

2. EXPERIMENT

During experiments in recent years, it was noted that the channel freezes very rarely even in cold winters. Strong currents of water with almost freezing temperature do not freeze in the channel to approximately a distance of 100 m from the channel along a narrow (~1-2 m) strip. Field works were performed in 2019 in Lake Valunden (Spitsbergen) near the channel connecting the lake with the fjord. A narrow (~1-2 m) strip of water in the continuation of the flow from the strip does not freeze (Fig. 2).

Fig. 2. Photo of the ice-free strip continuing the flow from the channel.

We found that ice thickness at the end of this strip was greater than in the lake. The mean ice thickness over the entire basin of the lake was approximately 70 cm. The ice near the end of the ice-free strip was thicker than 100 cm.

We performed a survey of ice thickness in the lake to make a detailed map of the ice thickness. The survey was made by drilling holes in the ice and measuring ice thickness with a graduated rod. The geographical coordinates of each point of measurements of ice thickness were taken using a GPS device with an accuracy of 1-2 m. It was found that ice thickness in the continuation of the ice-free jet and around it was greater than in the lake far from the channel. The survey showed that the characteristic size of the region, in which ice thickness was greater is of the order of ~100 m. The region of thicker ice is located immediately near the end of the non-freezing tidal stream. Here, the maximum ice thickness reached 120 cm. Ice thickness along the sides of the ice-free strip sharply increases from the ice-free water to 80-90 cm and then gradually decreases to 70 cm, which is typical for the ice thickness throughout the lake. A map of ice thickness based on our measurements is shown in Fig. 3.

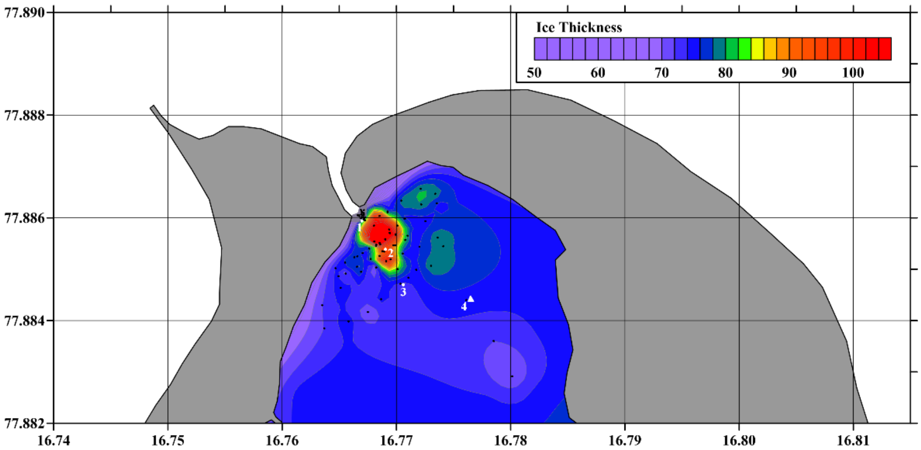

Fig. 3. Map of ice thickness in the lake (cm). Black dots show the locations of ice thickness measurements. Numbers (1-4) show locations of ice sampling for the tests.

Velocity of the flow from the channel was measured using a down-looking ADCP instrument fixed under ice at point 1 (Fig. 3). Magnitude of velocity changes with the tidal period. The maximum velocities exceed 1.5 m/s. A graph of time variation in the magnitude of velocity is shown in Fig. 4.

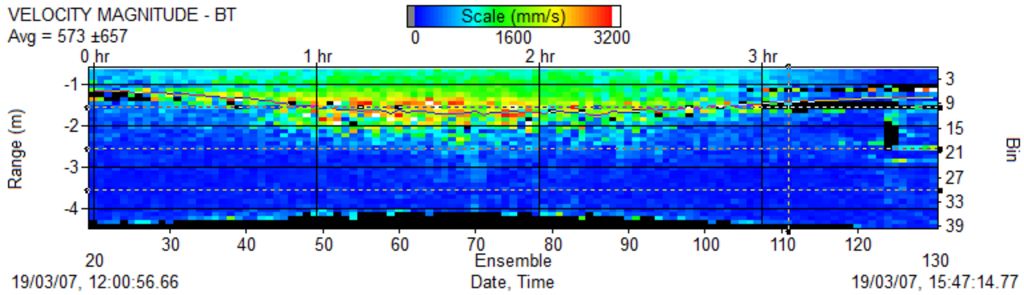

Figure 4. Magnitude of water velocity recorded with ADCP at point 1.

We suggest the following interpretation of this phenomenon. When water flows in the ice-free channel, the water temperature drops almost to the freezing point. Ice crystals and larger frazil ice particles are formed on the surface of the stream. Then, the near-freezing water flows under the ice and ice crystals and frazil ice attach to the already frozen ice sheet in the lake. When drilling holes in the continuation of the ice-free jet we found that the ice cover is not uniform as in the lake but consists of several layers.

3. MEASUREMENTS OF ICE STRUCTURE AT DIFFERENT LOCATIONS

We investigated the granular structure of ice at four locations at different distances from the channel. Vertical and horizontal sections made of sea ice cores taken from Locations 1-4 (Fig. 3) are shown in Figs. 5-8. Black strip corresponds to 5 cm length in the figures. Figures 5-8 show transformation of grain structure of sea ice over 300 m caused by the influence of tidal jet on the ice formation. Typical grain structure of ice in the lake far away from the tidal jet is shown in Fig. 5. The thin sections were produced from the ice core taken at Location 4 at the distance of about 300 m from the channel (Fig. 3). The ice structure belongs to S2 type with a typical diameter of ice columns of 2-3 cm. The columnar ice was formed in relatively calm sea water due to the atmosphere cooling. Such ice was observed at different locations of the lake over several years.

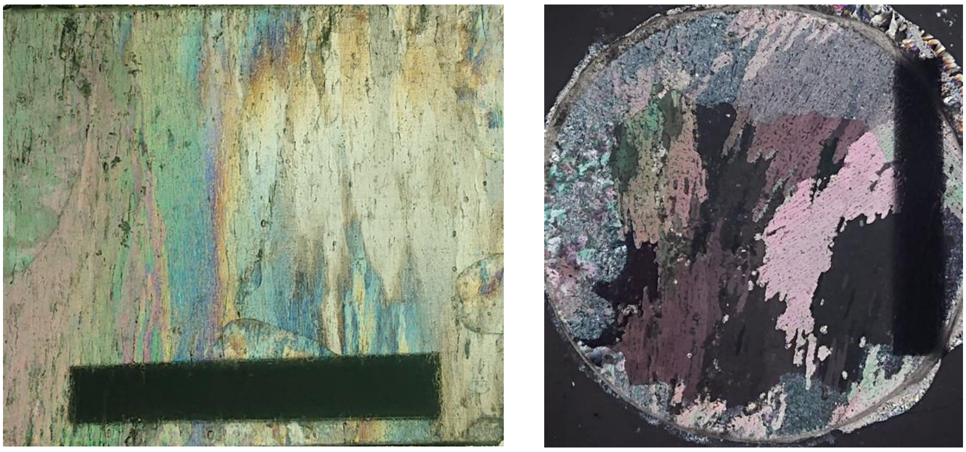

Figure 5. Vertical (left panel) and horizontal (right panel) thin sections of natural ice at point 4.

Figure 6 shows thin sections made from the ice cores taken at Location 3 at a distance of 200 m from the channel (Fig. 3). Ice columns are seen only on the vertical thin section taken from a depth of 20 cm from the ice top of the ice cover (bottom left panel in Fig. 6). Grain size of the horizontal thin section ranges within 0.5 cm to 1 mm (bottom right panel in Fig. 6). Deeper layers of ice have granular structure with smaller grains (top panel in Fig. 6). Vertical sizes of grains are slightly bigger than their horizontal sizes.

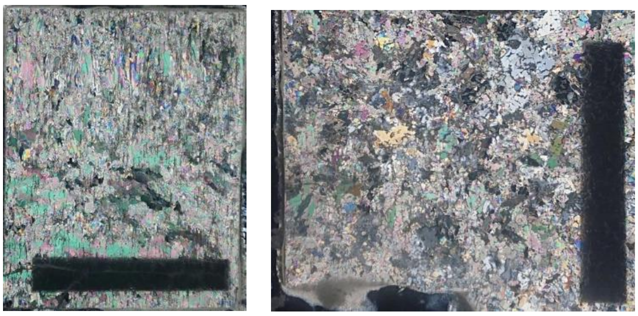

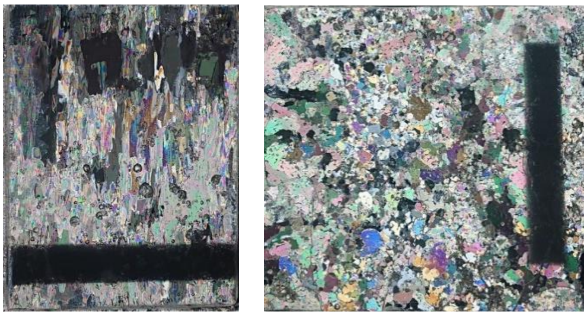

Figure 6. Vertical (left panel) and horizontal (right panel) thin sections of ice at point 3 taken from ice sample located in 20 cm from the bottom of the ice cover (top panel) and 20 cm from the top of the ice cover (bottom panel).

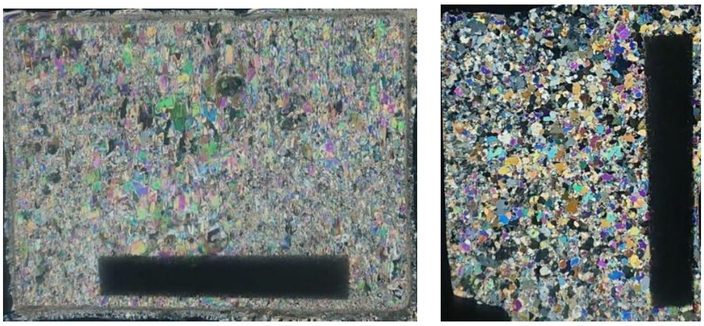

Figure 7. Vertical (left panel) and horizontal (right panel) thin sections of ice at point 2 taken from ice sample located in 20 cm from the ice bottom.

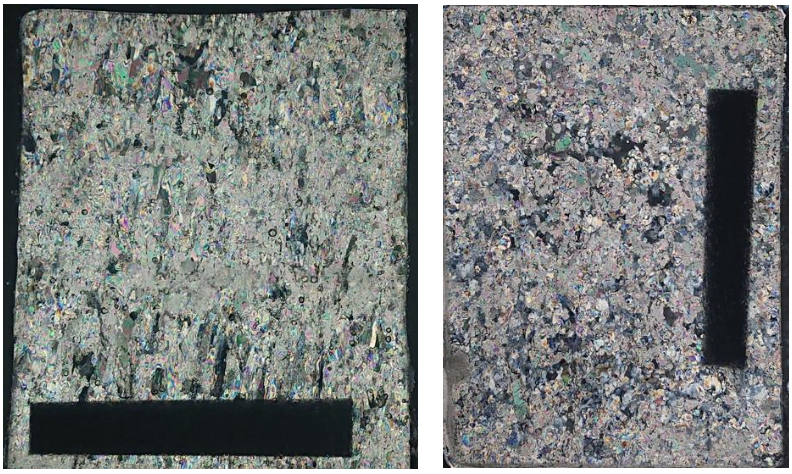

Figure 8. Vertical (left panel) and horizontal (right panel) thin sections of ice at point 1.

Figures 7 and 8 show that ice near the channel also has granular structure. Grain sizes at Location 1 are smaller than grain sizes at Location 2, and grain sizes at Location 2 are smaller than grain sizes at Location 3. We think that the revealed changes of ice structure are related to the increase of the turbulence in the water below the ice as the distance to the channel decreases. It is known that turbulence influences supercooling of water and formation of frazil ice [Omstedt, 1985; Clark and Doering, 2006]. Tide jet penetrates into the lake with a high speed up to 3 m/s (Fig. 4) and transports water from the fjord to the lake. Based on the data in 2018 salinity of sea water in the fjord is 34.40-34.45 PSU, while in the lake it is greater (34.72-34.75 PSU) [Morozov et al., 2019]. At the same time sea water in the lake and in the fjord are at their freezing points. Their mixing influences supercooling in the region where tidal jet interacts with sea water in the lake.

Supercooling leads to the formation of frazil and formation of granular ice. Freezing of freshwater flow from a glacier to the fjord was considered in [Marchenko et al, 2017; Morozov et al., 2015]

4. MODEL

To model the distribution of the inflowing cold water over the lake a system of regularized shallow water equations described in [*Bulatov and Elizarova*, 2011] has been used for numerical simulation together with a simplified model of the passive scalar transport [*Elizarova and Ivanov*, 2020]

$$\frac{\partial h}{\partial t} + \mathrm{div}\left(h(\vec{u} - \vec{w})\right) = 0, \tag{1}$$

$$\frac{\partial h\vec{u}}{\partial t} + \mathrm{div}(h(\vec{u} - \vec{w}) \otimes \vec{u}) + \vec{\nabla}\frac{gh^2}{2} = \left(h - \tau \mathrm{div}(h\vec{u})\right)\left(\vec{f_C} - g\vec{\nabla}b\right) + \mathrm{div}\Pi, \tag{2}$$

$$\frac{\partial Ch}{\partial t} + \mathrm{div}\left(Ch(\vec{u} - \vec{w})\right) = \mathrm{div}\left((D + \delta\tau gh)h\vec{\nabla}C + \tau\vec{u}h\left(\vec{u}\cdot\vec{\nabla}C\right)\right). \tag{3}$$

Here we use standard designations for shallow water model: h and $\vec{u} = \{u_x, u_y\}$ are water depth and horizontal velocities vector respectively, b describes the bathymetry, $g = 9{,}81$ m/s^2 is acceleration due to gravity, $\vec{f_C} = 2\Omega \sin\varphi \cdot \{u_y, -u_x\}$ is the Coriolis force, where $\Omega = 7.2921\ 10^{-5}$ s^{-1} is the angular velocity of the Earth's rotation and φ = 77.87° is latitude, which was assumed constant in the entire domain of simulation. Additional regularizing τ terms have the form of second spatial derivatives and dissipative character, where $\tau > 0$ is regularization parameter, whose dimension is time.

The goal of the simulation was to calculate currents in the lake during a tidal flow into the lake from the fjord. The transport equation was used for a simplified model of this process, in which the inflowing water of low temperature was considered as an "impurity". In this case, the distribution of the "impurity" concentration C can be compared with the thickness of the ice, which grows in the lake during the cold season and turns out to be thicker near the flow from the channel compared to its thickness in the entire lake. Concentration C is specified in dimensionless units.

Since we consider cold water transport, it can be assumed that function C is the temperature, and D is the coefficient of thermal diffusivity of water. This coefficient is very small (at 0°C, $D \approx 13.2 \cdot 10^{-8}$ m^2/s); therefore, it can be neglected. The currents in the lake are low (about 10 cm/s); therefore, the regularizer on the right-hand side of Eq. (3), represented by the dissipative term of the order of $\sim\tau hu^2$, is insufficient to ensure the stability of the numerical solution. That is why an artificial term $\delta\mu = \delta\tau gh$ was introduced to coefficient D in the transport equation (3) of the model, where δ is a dimensionless coefficient chosen from the conditions of stability and calculation accuracy, and $\mu = \tau gh$ is the artificial coefficient of kinematic viscosity of fluid.

Bathymetry of the lake was constructed using the following model (Fig. 9): the water depth in the inlet channel is 1 m, the channel width is approximately 10–12 m, the length of the entire channel is approximately 200 m, the depth of the lake is 10 m, and the height of the banks above the lake is 2 m.

The following boundary conditions were set to simulate the flow of cold water into the lake, at the boundary of the channel flowing into the lake (x = 1300 m), where t is given in hours

$$\frac{\partial h}{\partial y} = 0, \qquad u_y = -\sin\left(\frac{\pi t}{6}\right) m/s, \qquad u_x = 0\ m/s, \qquad C = 1.$$

For an accurate simulation of the water motion near the coastal zone, a special dry-bed condition was used. A similar problem without taking into account the propagation of impurities was considered using the system of regularized shallow water equations; its solution, as well as a description of the method for calculating the zones of flooding/drying, are given in [*Bulatov and Elizarova*, 2016].

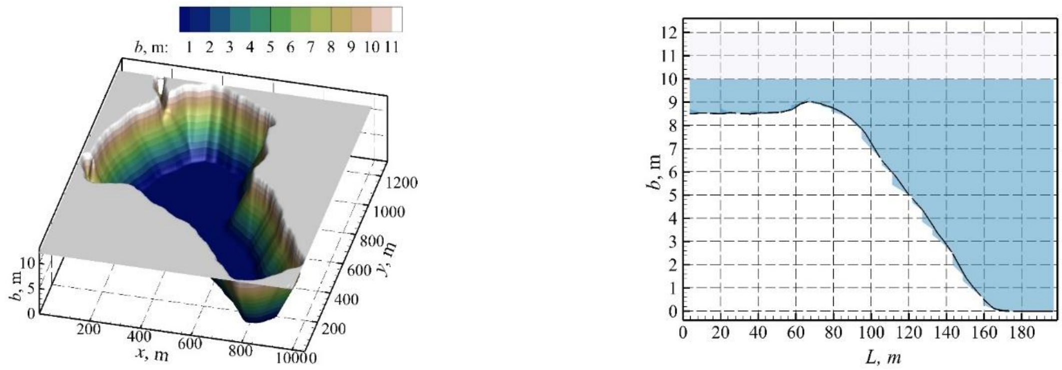

Fig. 9. (a) Lake bathymetry model; (b) the location of the channel entrance into the lake over the section, L is the distance along the channel axis, the water level is indicated in blue (ξ = 10 m).

The first-order Euler scheme for time derivatives and second-order scheme for spatial derivatives were used for the numerical solution of the system of equations (1) - (8). A uniform rectangular grid with the following parameters was used:

$$N_x = 247, \Delta x = 4.1 \text{ m};$$

$$N_y = 234, \Delta y = 5.4 \text{ m};$$

$$\alpha = 0.3, \delta = 0.1, \varepsilon = 0.01 \text{ m}.$$

The time step was chosen in accordance with the Courant–Friedrichs–Lewy condition:

$$\Delta t = \beta \frac{(\Delta x + \Delta y)}{2\sqrt{g h_{max}}}, \qquad \beta = 0.2.$$

Figure 10 shows the pattern of the flow and streamlines of the absolute value of velocity $|u| = \sqrt{u_x^2 + u_y^2}$ over a time period of 3h, which corresponds to the maximum velocity of water flow into the lake. The distribution of the velocity (of the order of several centimeters per second) far from the channel is consistent with the field measurements [Morozov et al., 2019]. A pattern of the formation of a circular cyclonic eddy with a diameter of 200-300 m is seen, which is also consistent with observations.

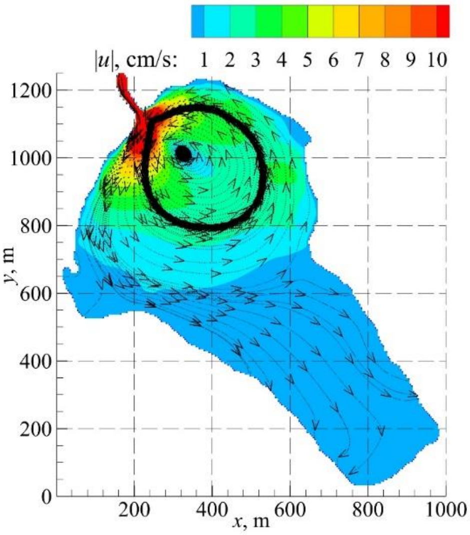

Fig. 10. Circulation in the lake, and streamlines of the absolute value of velocity $|u|$ at t = 3 h, when the velocities of the flow into the lake are maximum.

Proportion of the cold water flowing from the channel to that in the lake determines the formation of ice around the ice-free jet. An eddy of circulating water is formed near the channel. Various versions of the numerical experiments have shown that the Coriolis force does not influence this eddy. The form of circulation is caused solely due to the shape of the lake and the position of the inflow. The Coriolis force does not have influence because of the small spatial scale of the phenomenon and size of the lake. The effect of the Earth's rotation becomes important when the time scales of the motion are comparable with the inertial period. The inertial period at latitude 78º N is ~12 h. The size of the eddy in the lake is of the order of ~100 m and the velocity of the current in the lake is of the order of ~0.1 m/s. Hence, the time scale is of the order of ~1000 s, which is much smaller than the inertial period here. Cold water is concentrated near the outflow from the channel to the lake (Fig. 11) and almost does not spread further. Hence, the region of thicker ice coincides with the size of the circulation eddy.

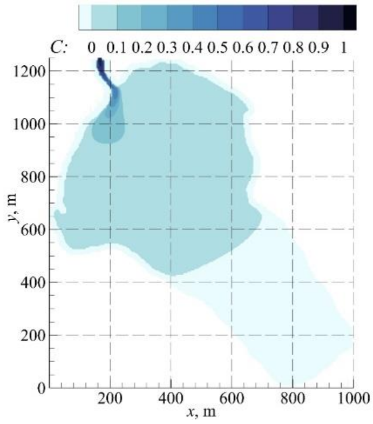

Fig. 11. Distribution of concentration C in the lake at time moment t = 3 h.

Figure 12 shows the maps of ice thickness the eddy and concentration distribution based on the model simulations. Ice thickness is greater in the region located close to the channel. Here, a cyclonic eddy is formed by the inflowing tidal flow. The size of the region of thick ice is the same as the region if high velocities near the channel as well as the size of the region of impurity (very cold water) in Fig. 11.

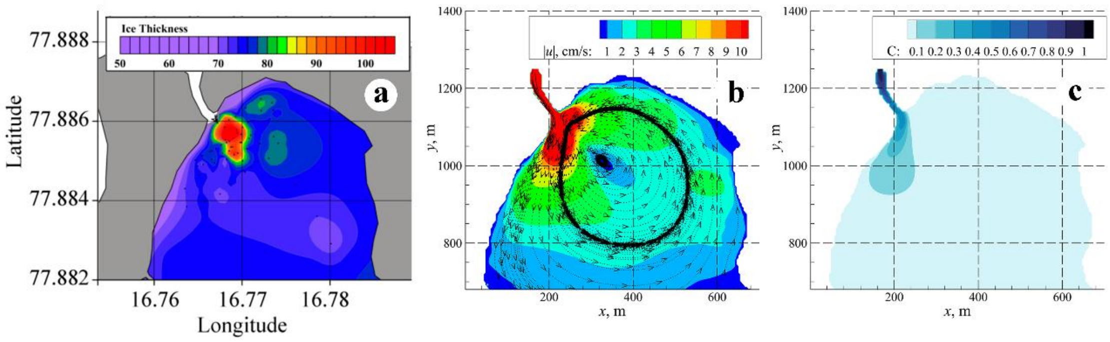

Fig. 12. Combined maps of ice thickness (a); lake currents simulation (b) and model cold water distribution. Cyclonic eddy is highlighted with a bold black line.

CONCLUSIONS

A survey of ice thickness in Lake Valunden showed that ice thickness near the tidal jet flowing from the Van Mijen Fjord to Lake Vallunden and in the continuation of this jet is greater than over the entire lake. The ice-free flow from the channel was about 1-2 m wide and 50-100 m long. Very cold, supercooled water flows under ice transporting ice crystals and slash. Due to the decrease in the velocity of the jet, the ice crystals attach to the bottom of the ice cover increasing ice thickness in the continuation of the flow. A numerical model simulation resulted in a chart of currents in the lake induced by the tidal current. The flow forms eddies expanding over the basin of the lake with decreasing velocities.

Tidal jet influences regular mixing of waters from the fjord and lake and supercooling of the fjord water. Supercooling of the fjord water leads to frazil formation. Granular structure of sea ice within a region of about 200 m in size near the channel is explained by the freezing of frazil ice dominating over thermal growth of columnar sea ice.

ACKNOWLEDGEMENTS

This research was supported by the Norwegian Research Council (NFR) (project no. 196138/S30) and by the State Task of the Shirshov Institute of Oceanology (0128-2021-0002) and Russian Foundation for Basic Research (project nos. 20-08-00246 and 19-01-00262).

REFERENCES

Bulatov O.V., Elizarova T.G. 2011. Regularized shallow water equations and an efficient method for numerical simulation of shallow water flows. *Computational Mathematics and Mathematical physics* 18(1). pp. 170–184.

Bulatov O.V., Elizarova T.G. 2016. Regularized shallow water equations for numerical simulation of flows with a moving shoreline. *Computational Mathematics and Mathematical physics 56 (4)*.665–684.

Clark S., Doering J.C. 2006. Effect of turbulence intensity on frazil formation. Proc. of 18th IAHR International Symposium on ice, pp. 267-275.

Elizarova T.G., Ivanov A.V. 2020. Numerical simulation of the transport of a passive scalar in shallow water using a quasi-gas-dynamic approach. *Computational Mathematics and Mathematical Physics 60 (7)*. pp. 1248–1267.

Marchenko A.V., Morozov E.G. 2013. Asymmetric tide in Lake Vallunden (Spitsbergen), *Nonlinear Processes in Geophysics 20*. pp. 935-944.

Marchenko A.V., Morozov E.G. 2016. Seiche oscillations in Lake Valunden (Spitsbergen), *Russ. J. Earth. Sci. 16*, ES2003, doi:10.2205/2016ES000567.

Marchenko A.V., Morozov E.G., Marchenko N.A. 2017. Supercooling of seawater near the glacier front in a fjord, *Journal of Earth Science Research (Canada*), 6(1), pp. 97-108.

Morozov E.G., Pisarev S.V. 2002. Internal tides at the Arctic latitudes (numerical experiments), *Oceanology,* 42(2), pp. 153–161.

Morozov E.G., Marchenko A.V., Filchuk K.V., Kowalik Z., Marchenko N.A., Ryzhov I.V. 2019. Sea ice evolution and internal wave generation due to a tidal jet in a frozen sea, *Applied Ocean Research 87*. pp. 179-191.

Morozov E.G., Marchenko A.V., Fomin Yu.V. 2015. Supercooled water near the glacier front in Spitsbergen, *Izvestiya, Atmospheric and Oceanic Physics*, 51 (2), pp. 203–207.

Omstedt A. 1985. On supercooling and ice formation in turbulent sea-water. *J. Glaciology*, 31(109), pp. 263-271.